Density functional study of multiferroic Bi_2NiMnO_6

Adrian Ciucivara,[1] Bhagawan Sahu,[2] and Leonard Kleinman[1]
[1]*Department of Physics, University of Texas at Austin, Austin, Texas 78712-0264, USA*
[2]*Microelectronics Research Center, University of Texas at Austin, Austin, Texas 78758, USA*
(Received 13 March 2007; revised manuscript received 17 May 2007; published 10 August 2007)

Using both the generalized gradient approximation (GGA) and GGA+U density functionals and including the spin-orbit interaction while allowing for noncollinear spin orientations, we have calculated many of the properties of the multiferroic Bi_2NiMnO_6. The GGA and GGA+U results are in unexpectedly close agreement; in particular, their lattice constants are in excellent agreement with the measured values. The calculated GGA and GGA+U magnetizations per formula unit are 4.92 and 4.99 μ_B and the calculated ferroelectric polarizations are 16.84 and 16.63 $\mu C\,cm^{-2}$. A discussion is given of the $C2$ space group of Bi_2NiMnO_6 and of the centrosymmetric $C2/m$ space group from which it can be generated with small atomic displacements.

DOI: 10.1103/PhysRevB.76.064412 PACS number(s): 75.50.Dd, 77.84.−s, 75.50.Pp

I. INTRODUCTION

Ferromagnetic ferroelectric multiferroic materials appear to have great potential for device applications. If the magnetization M and the electric polarization P are uncoupled, they can be used to encode four different logic states. For example, Gajek *et al.*[1] have reported using 2 nm thick films of $La_{0.1}Bi_{0.9}MnO_3$ as spin filtering tunnel barriers, the magnetization and electric polarization of which can be switched independently, giving rise to four different resistance states. There has been much effort expended to find strongly coupled systems. There has been some success in inducing a reversal of the electric polarization[2,3] with a magnetic field, but thus far, as far as we know, only suggestions[4] exist for reversing the magnetization with an electric field. Fennie and Rabe[5] have demonstrated theoretically that epitaxially strained $EuTiO_3$ can be switched from its antiferromagnetic-paraelectric phase to a ferromagnetic-ferroelectric phase with the application of either an electric or magnetic field, but that the direction of the magnetization cannot be reversed in this case by an electric field.

There exist relatively few magnetoelectric multiferroics, and most of those are antiferromagnetic. They form a fascinating field of study which can be framed by two questions asked by Hill and co-workers[6–8] and Ederer and Spaldin.[9] "Why are there so few magnetic ferroelectrics?" "Why are there any magnetic ferroelectrics?" Covalent bonding between the transition metal (TM) d and the oxygen $2p$ electrons in the ferroelectric perovskites destroys any possibility of magnetism and seems to be essential for stabilizing the ferroelectric distortion.[6] There does not seem to be any disagreement with this explanation but our interpretation of the nature of the covalent bond and how it suppresses magnetism[10] differs from that of Spaldin. Seshadri and Hill[8] argued that the large distortion in multiferroic $BiMnO_3$ is not due to TM-O bonding but rather due to the Bi moving away from a site with inversion symmetry in order to allow its $6s$ and $6p$ electrons to hybridize with each other. This idea actually had been proposed[11] as long ago as 1968. Somewhat later, Hill and Filippetti[7] noted that tight binding calculations indicate that it is Bi-O covalency that drives the distortion, but they[7,12] still suggested that it is the stereochemical activity of the Bi $6s^2$ lone pair that causes the structural distortion. Shishidou *et al.*[13] pointed out that the Bi $6s$ states can hardly play any positive role since they are fully occupied and at a very deep binding energy. They attributed the distortion to strong hybridization between Bi $6p$ and O $2p$ states. Other explanations have been given[7,14] for $YMnO_3$, a prototypical hexagonal antiferromagnetic ferroelectric rare earth manganite, but we shall limit our further discussion to the distorted ferromagnetic perovskites.

Very recently, Belik *et al.*,[15] using selected area and convergent beam electron diffraction, found that bulk $BiMnO_3$ crystallizes in the centrosymmetric space group $C2/c$. Montanari *et al.*[16] agree with this result. This, if correct, overturns the many previous results[15] that found that the structural phase transition at $T_E \sim 450$ K was to the noncentrosymmetric $C2$ ferroelectric structure.[17] Belik *et al.* suggested that measured dielectric hysteresis loops were due to nonlinear dielectric losses rather than ferroelectricity and that the observation of reflections characteristic of the $C2$ space group was due to double diffraction. They also considered it possible that impurities or poor stoichiometry could cause $BiMnO_3$ to crystallize in the $C2$ space group. They found a magnetization of 3.92 μ_B/f.u. at 5 K with a 5 T field but almost no remnant magnetization and a Curie temperature of $\sim$100 K. A local spin density approximation (LSDA) calculation[12] found $BiMnO_3$ to be a metal, but with a Hubbard $U-J$ of 6.94 eV, a gap opened up and a Berry phase[18] calculation yielded $P=0.52\ \mu C\,cm^{-2}$, an order of magnitude larger than the experimental values. Among the handful of other ferromagnetic ferroelectrics, $BiFeO_3$ may be the most interesting, both because of its high transition temperatures and its thin film properties.[19] Bulk samples become antiferromagnetic (with a very small ferromagnetic component due to spin canting) at $T_N \sim 643$ K and ferroelectric at $T_E \sim 1103$ K with a spontaneous polarization of 6.1 $\mu C\,cm^{-2}$ at 77 K. In a thin film, a remnant polarization of 50–60 $\mu C\,cm^{-2}$ was obtained. A saturation magnetization of $\sim 1\ \mu_B$/unit cell was obtained with a 70 nm film (with a negligible remnant magnetization). The saturation magnetization was very dependent on film thickness, dropping to $\sim 0.03\ \mu_B$ in a 400 nm film. Yun *et al.*[20] reported remnant polarizations of 73 $\mu C\,cm^{-2}$ at room temperature and 146 $\mu C\,cm^{-2}$ at 90 K in 350 nm films. The thin film has a

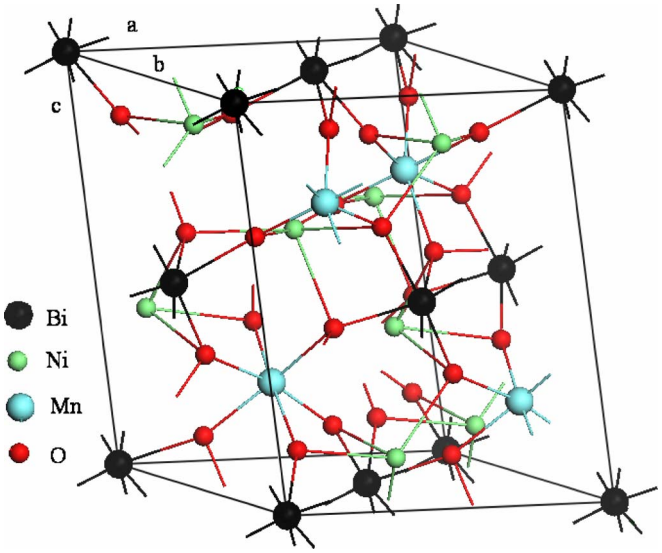

FIG. 1. (Color online) Unit cell of Bi_2NiMnO_6 containing 4 f.u.

tetragonal structure, while bulk $BiFeO_3$ is rhombohedral. Interestingly, Neaton *et al.*[21] performed LSDA+U Berry phase calculations for the bulk structure and obtained thin-film-like polarizations of 90–100 $\mu C/cm^2$, depending on the parameter U.

Recently, Bi_2NiMnO_6 has been synthesized[22] as a heavily distorted double perovskite with 4 f.u. in a monoclinic unit cell, as shown in Fig. 1. The magnetization measured at 5 K was 4.1 μ_B/f.u. at 5 T. That this was less than 5 μ_B was attributed to a small amount of Ni-Mn antisite disorder. The residual magnetization, if any, was too small to be discernable in their Fig. 3. Unfortunately, T_M=140 K, well below room temperature, making it unlikely that Bi_2NiMnO_6 will have any practical applications, while T_E=485 K is fairly low but still well above room temperature. A very recent thin film measurement[23] yielded a saturated magnetization of 4.5 μ_B and a saturated polarization of about 5 $\mu C/cm^2$ at 7 K. The only calculation[24] of which we are aware assumed a cubic double perovskite structure with an 8 Å lattice constant for this highly distorted crystal, so that the comparison we shall make with their results is not expected to result in agreement. We have performed electronic structure calculations for Bi_2NiMnO_6 using both the generalized gradient approximation (GGA) and GGA+U density functionals. In the next section, we describe our computational method and discuss the crystal symmetry, which will give insight into the nature of the electric polarization. In the third section, our results are given and compared with experiment.

II. COMPUTATIONAL METHOD AND CRYSTAL SYMMETRY

Density functional calculations were performed using the projected augmented wave[25] method as implemented in the VASP code.[26] The Perdew-Burke-Ernzerhof form[27] of the generalized gradient approximation was used, both without and with a Hubbard U. We took $(U-J)_{Mn}$=3.5 eV and $(U-J)_{Ni}$=4.0 eV, assuming that values used elsewhere[28,29] to obtain agreement with experiment are transportable to this situation.[30] Because Bi plays an important role in multiferroics and it is the heaviest nonradioactive atom, we thought it appropriate to include the spin-orbit interaction, and since the orientation of **M** relative to **P** is of interest, we allowed the magnetization to be noncollinear. Because we were already using spinor wave functions, this incurred very little extra computational cost. Unfortunately, this precludes us from making orbital projections of the density of states (DOS) but does allow projections of the charge and Cartesian components of the magnetization within inscribed spheres. From a Curie-Weiss fit to the magnetic susceptibility, an effective Mn moment of 4.69 (4.79) μ_B at low (high) temperature was obtained[15] for $BiMnO_3$ although the measured magnetization was 3.92 μ_B/f.u. If the atomic moments obtained from Curie-Weiss are meaningful, they must be noncollinear, which gives an additional rationale for allowing for noncollinearity in Bi_2NiMnO_6. In order not to prejudice the magnitude or direction of **M**, we started with the magnetization on the four Mn in the (001), (00−1), (010), and (0−10) directions with magnitude of 3 or 5 μ_B. The other atoms (including Ni) were given polarizations of (0,0,0.01) and (0,0,−0.01) μ_B. A $4\times8\times4$ **k**-point sample of the Brillouin zone was used. The Bi 5d and Mn 3p outer core electrons were treated as valence electrons. The basis sets contained all plane waves up to 18.9 Ry. The atomic forces were reduced to less than 10 meV/Å or, equivalently, until the total energy was converged to 10^{-4} eV per 40 atom unit cell.

TABLE I. The number of positions and Wyckoff notation for symmetry points in the unit cell of the $C2$ space group and the points in the centrosymmetric $C2/m$ space group from which they differ by displacements along the **a**, **b**, and **c** lattice vectors. The third column lists the positions of half the atoms in each set of points. The other half are obtained by an $(a/2,b/2,0)$ translation. When the displacements indicated by Greek letters vanish, $C2$ becomes $C2/m$.

$C2$	$C2/m$	Positions
2a	2a	$(0,\alpha,0)$
2b	2d	$(\frac{1}{2},\beta,\frac{1}{2})$
4c	4i	(x,γ,z) $(-x,\gamma,-z)$
4c	8j	$(x,y-\delta,z)$ $(-x,y-\delta,-z)$
4c		$(x+\mu,-y,z+\eta)$ $[-(x+\mu),-y,-(z+\eta)]$

Figure 1 is the monoclinic unit cell containing 4 f.u. of Bi_2NiMnO_6 with space group $C2$ (No. 5). The short axis is the **b** lattice vector which is perpendicular to the **a** and **c** vectors which make an angle β with each other. In Table I, the allowed positions of the atoms in the unit cell are tabulated according to the number of positions at each symmetry point and its Wyckoff label. The Greek letters signifying displacements along the lattice vectors are assumed to be relatively small and when they all vanish, the space group becomes the centrosymmetric $C2/m$ (No. 12). The twofold rotation about **b** is easily seen. For the 2a and 2b sites, the atoms go into themselves, mod a lattice translation. For the

TABLE II. GGA and GGA+U values of Bi_2NiMnO_6 lattice constants and angle compared with experiment (Ref. 20) and cohesive energy per 40 atom unit cell.

	a (Å)	b (Å)	c (Å)	β (deg)	E_c (eV)
GGA	9.501	5.418	9.634	107.884	264.50
GGA+U	9.557	5.447	9.680	107.848	263.67
Expt.	9.465	5.423	9.543	107.823	

4c sites, pairs of atoms are interchanged by the rotation. Thus, the electric polarization must lie along **b**. Note that the 4c's are of two different types, those emanating from 4i and those emanating from 8j. When γ=0, the 4ci sites go into themselves under a reflection in the **b** plane and into each other under inversion, but when μ, η, and δ=0, under either reflection or inversion the 4cj sites within a single 4c do not transform amongst themselves, but rather into sites in the other 4c.

III. RESULTS

In Table II, the calculated lattice constants and angle are compared with experiment. The agreement is excellent, with the GGA lattice constants being in better agreement with experiment than GGA+U but the GGA+U angle being in better agreement with experiment. The cohesive energy, amounting to about 6.6 eV per atom, is also given. A cohesive energy of this magnitude is indicative of strong covalent bonding. The effect of U on the total crystal energy is to reduce it by 6.27 eV; but because its effect on the atoms is similar to its effect on the crystal, it only reduces the cohesive energy per 40 atom unit cell by 0.83 eV. In Table III, the atomic positions within the unit cell are compared. The GGA and GGA+U agree well with each other but not as well with experiment. We think that this may be a case where the theoretical results are more accurate than the experimental results. It seems unlikely that such accurate values for the lattice constants and angle could be obtained with sizable errors in the atomic positions. On the other hand, the experimental atomic positions were obtained by fitting the x-ray scattering factors with a superposition of ionic charge densities, including Ni^{2+} and Mn^{4+}. It is unlikely that fitting the charge density of a covalent crystal in this manner will lead to an accurate placement of the atoms. Figure 2 is a plot of the GGA and GGA+U total DOS. (VASP is unable to obtain a spin DOS from a spin-orbit calculation.) The GGA (GGA+U) energy gap is 0.448 eV (0.493 eV). The bonding Bi 6p, Mn and Ni 3d, and O 2p bands are over 6 eV wide and the 16 Bi 6s bands are almost 2 eV below them.

The first three columns of the first five rows of Table IV are sums of the components of the magnetization in μ_B/f.u. projected[31] on each kind of atom. The variation among atoms of a particular kind was negligible (except for the oxygen atoms, whose individual contributions are small) in the GGA+U and small in the GGA except the GGA calculation resulted in the Ni 2a and 2b sites having similar magnitudes but different directions of magnetic polarization. Here, x and y are the **a** and **b** lattice vector components and z is the third Cartesian component (not along **c**). M is the magnitude of those projected components of magnetization, n is the number of electrons in each set of spheres, and the last two columns, $n \pm M$, are the projected numbers of majority and minority spins. The row labeled P_T contains the sum of the above except for M, which is the magnitude of the sums of the components, rather than the sum of the magnitudes. Note that although the projection spheres[31] encompass only 59% of the unit cell volume (in the GGA case), they contain 86% of its electronic charge and 97% of its magnetic moment. The Mn sphere contains 5.6 electrons, implying an ionicity of no more than 1.4+ rather than the 4+ required if the oxygen were given its nominal 2− ionicity. Ionicity is an ill defined quantity, depending on how the charge outside the spheres is assigned and, more importantly, on the values chosen for the radii of the spheres. We note that our oxygen

TABLE III. Calculated atomic positions. For every 4c site listed at (xyz), there is another at ($-x,y,-z$) and then for every site there is another at $\left(x+\frac{1}{2},y+\frac{1}{2},0\right)$. Here, x, y, and z refer to distances along the crystal axes and not to Cartesian coordinates. The first set of O's emanate from 4i and the second set from 8j in Table I.

		GGA			GGA+U			Expt.		
Atom	Site	x	y	z	x	y	z	x	y	z
Ni	2a	0.000	0.000	0.000	0.000	0.000	0.000	0.000	0.000	0.000
Ni	2b	0.500	0.030	0.500	0.500	0.032	0.500	0.500	0.015	0.500
Mn	4c	0.252	0.013	−0.251	0.252	0.013	−0.251	0.243	0.013	−0.251
O	4c	0.094	−0.042	−0.166	0.093	−0.043	−0.167	0.111	−0.061	−0.151
O	4c	0.414	0.056	−0.332	0.414	0.064	−0.331	0.420	0.042	−0.320
Bi	4c	0.135	0.016	0.375	0.137	0.017	0.378	0.133	−0.023	0.378
Bi	4c	0.373	0.042	0.125	0.372	0.042	0.124	0.364	0.035	0.123
O	4c	0.162	0.296	−0.370	0.162	0.299	−0.369	0.146	0.276	−0.364
O	4c	−0.154	−0.205	0.410	−0.156	−0.204	0.410	−0.157	−0.258	0.413
O	4c	0.356	0.220	−0.094	0.355	0.223	−0.092	0.377	0.204	−0.111
O	4c	−0.342	−0.282	0.140	−0.341	−0.280	0.139	−0.338	−0.284	0.126

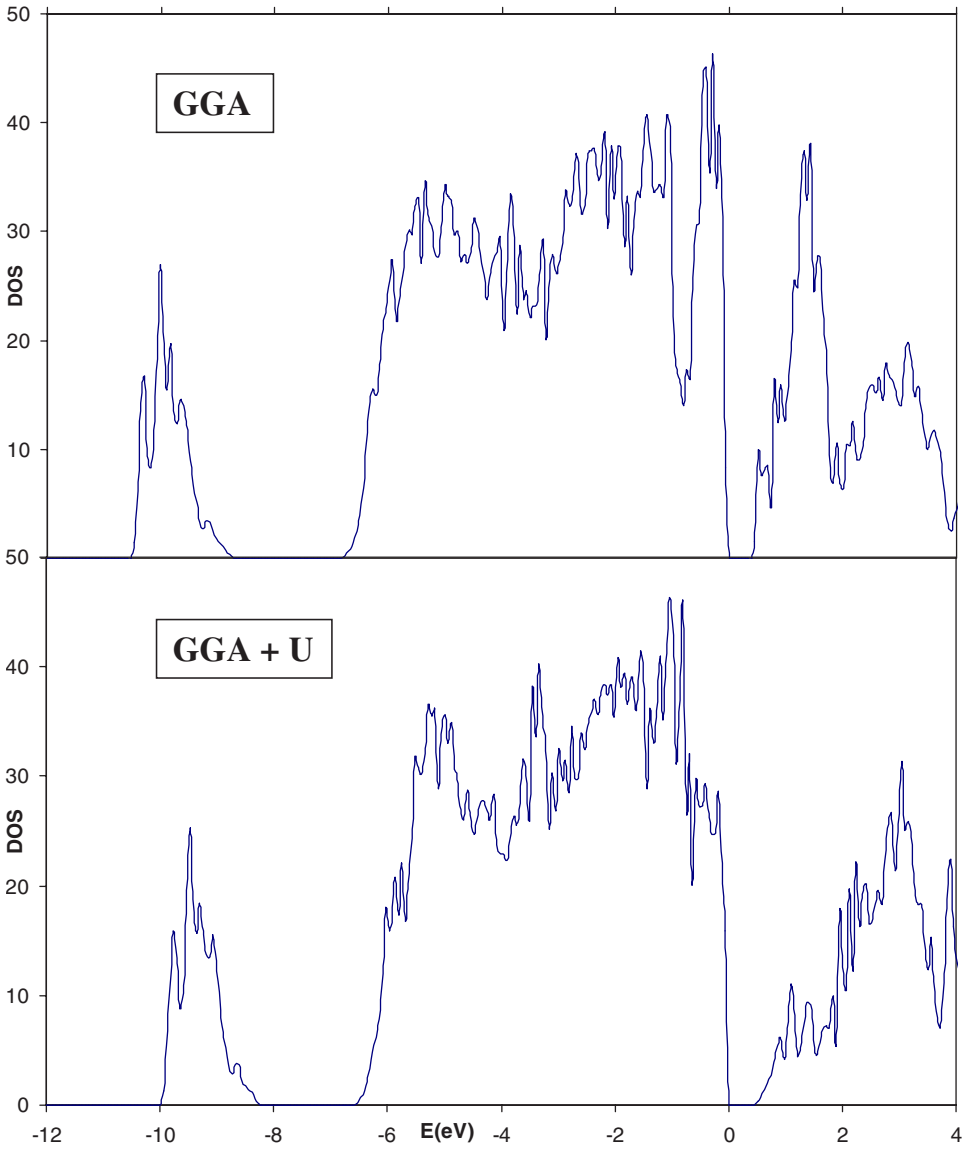

FIG. 2. (Color online) GGA and GGA+U DOS of Bi_2NiMnO_6 in states per unit cell per eV. The top of the valence band is taken at $E=0$.

radius of 0.900 Å is much larger than the 0.66 Å given[32] for the radius of covalently bonded oxygen. The last row, labeled Ξ_T, contains the actual (unprojected) values of the previously mentioned items.

The GGA+U result, $M=4.99\ \mu_B$, is in near perfect agreement (and the GGA in very good agreement) with the predicted[20] value of 5 μ_B in the absence of antisite disorder. However, that prediction was based on the assumption that

TABLE IV. Projections of the magnetic moments in μ_B/f.u. averaged over the Ni 2a and 2b sites and over the Mn, Bi, and O sites, the magnitude of those moments, the number of projected electrons, and the number of majority and minority spins on each kind of atom. P_T is the sum of those projected quantities and the row labeled Ξ_T lists those quantities evaluated over the entire crystal.

	GGA							GGA+U						
	x	y	z	M	n	$n^{\uparrow}$	$n^{\downarrow}$	x	y	z	M	n	$n^{\uparrow}$	$n^{\downarrow}$
2a Ni	0.252	0.446	0.508	0.721	4.130	2.425	1.704	0.469	0.462	0.453	0.799	4.126	2.462	1.663
2b Ni	0.471	0.424	0.336	0.718	4.129	2.423	1.706	0.467	0.461	0.454	0.797	4.125	2.461	1.664
Mn	1.481	1.767	1.715	2.874	5.616	4.245	1.371	1.948	1.938	1.921	3.353	5.511	4.432	1.079
Bi	0.028	0.033	0.032	0.054	4.973	2.514	2.460	0.024	0.024	0.024	0.042	4.978	2.510	2.468
O	0.223	0.263	0.260	0.434	35.216	17.825	17.391	−0.066	−0.066	−0.064	−0.113	35.260	17.686	17.573
P_T	2.454	2.933	2.850	4.800	54.064	29.432	24.632	2.841	2.820	2.788	4.878	53.999	29.552	24.447
Ξ_T	2.539	3.042	2.954	4.942	63.000	33.971	29.029	2.907	2.885	2.853	4.991	63.000	33.996	29.005

TABLE V. The GGA and GGA+U electric polarizations calculated at nine points from the original $C2$ structure, through the centrosymmetric $C2/m$ structure, to the inverted $C2$ structure. The last column, labeled ΔP, lists the polarization quanta.

	GGA	GGA+U
100%	16.839	16.625
75%	12.753	12.588
50%	8.443	8.342
25%	4.273	4.217
0%	0.000	0.000
−25%	−4.273	−4.217
−50%	−8.443	−8.342
−75%	−12.753	−12.588
−100%	−16.839	−16.625
ΔP	18.405	18.180

the manganese was Mn^{4+} with three majority and no minority spins, which is very far from the case here. The GGA and GGA+U magnetizations point in slightly different directions which are far from the rotation axis and far from perpendicular to it. Note that because Bi_2NiMnO_6 is a semiconductor, the deviation from an exact integer value for the magnetization (assuming $g=2$) is due to the spin-orbit interaction and the small noncollinearity of the spins. The effect of the Hubbard U is to increase the majority and decrease the minority spin on the Ni and Mn while slightly decreasing their total charge. This is done at the expense of the oxygens which have a net projected majority spin in the GGA but net minority spin in the GGA+U.

The Berry phases[16] were calculated for an 8×8 array of strings containing 16 **k** points to obtain the electric polarizations $\mathbf{P}'$ listed in Table V for a set of fractional displacements between +100% and −100% of the calculated displacements, α, β, γ, δ, μ, and η. (The energy gap exists for all values of the displacements.) Because of the periodic boundary conditions imposed on the infinite crystal, **P** is only defined mod a quantum of polarization $\Delta\mathbf{P}$, i.e., $\mathbf{P}=\mathbf{P}'+n\Delta\mathbf{P}$ with $\Delta\mathbf{P}=e\mathbf{b}/\Omega$, where e is the electronic charge, Ω is the unit cell volume, and **b** is the lattice vector. We note that when the displacements vanish, so does $\mathbf{P}'$ (there exist centrosymmetric cases[19] where $\mathbf{P}'=\frac{1}{2}\Delta\mathbf{P}$) and that $\mathbf{P}'$ varies approximately linearly with the displacements. The measured polarization is usually taken to be half of the difference between the positive and negative polarizations so $\Delta\mathbf{P}$ can be ignored in cases where the centrosymmetric polarization vanishes and our calculated polarizations are 16.839 μC cm^{-2} (GGA) and 16.625 μC cm^{-2} (GGA+U). These modest values are nevertheless large compared to the thin film experimental value of about 5 μC cm^{-2}, perhaps because the thin film crystallized in a tetragonal perovskite structure due to the constraining effect of its perovskite substrate. The relatively small magnitudes of $\mathbf{P}'$ and $\Delta\mathbf{P}$ are a consequence of **b** being much shorter than **a** and **c**. The local density approximation and GGA "cubic" calculations of Ref. 24 resulted in exactly 5 μ_B on Mn and 1 μ_B on Ni. Considering the hybridization, that these are exact integers is surprising. They also obtained $P=28$ μC/cm^2 and mentioned that this was remarkably greater than the 18 μC/cm^2 obtained from the point charge model. Although our results are much closer to the point charge model, we agree with them that the point charge model can have large errors. We note that the calculated magnetizations of the crystal and its enantiomorph were found to be identical, as they must be because **M** is a pseudovector and unchanged by inversion. In principle, if **P** could be rotated through 180°, **M** might follow. Rotating the polarization by rotating an electric field seems possible for simple perovskites which are cubic except for a small distortion caused by the polarization, but, unfortunately, these are not magnetic. Rotating the polarization in a truly uniaxial crystal might be done by rotating the crystal in a strong electric field. However, the coupling between **P** and **M** in Bi_2NiMnO_6 seems to be sufficiently weak that even if the **P** could be rotated through 180°, it is unlikely that **M** would follow. This conclusion was drawn from the fact that **M** in the centrosymmetric crystal was found to be negligibly different from **M** in Table IV. In the GGA+U case, for example, $\mathbf{M}=(2.923, 2.8773, 2.8494)$ μ_B.

ACKNOWLEDGMENTS

This work was supported by the Welch Foundation (Houston, Texas) under Grant No. F-0934 and by the Texas Advanced Computing Center. B.S. thanks NRI-SWAN for financial support.

[1] M. Gajek, M. Bibes, S. Fusil, K. Bouzehouane, J. Fontcuberta, A. Barthelemy, and A. Fert, Nat. Mater. **6**, 296 (2007).
[2] N. Hur, S. Park, P. A. Sharma, J. S. Ahn, S. Guha, and S.-W. Cheong, Nature (London) **429**, 392 (2004).
[3] T. Kimura, T. Goto, H. Shintani, K. Ishizaka, T. Arima, and Y. Tokura, Nature (London) **426**, 55 (2003).
[4] Ch. Binek and B. Doudin, J. Phys.: Condens. Matter **17**, L39 (2005).
[5] Craig J. Fennie and Karin M. Rabe, Phys. Rev. Lett. **97**, 267602 (2006).
[6] Nicola A. Hill, J. Phys. Chem. B **104**, 6694 (2000).
[7] Nicola A. Hill and Alessio Filippetti, J. Magn. Magn. Mater. **242-245**, 976 (2002).
[8] Ram Seshadri and Nicola Hill, Chem. Mater. **13**, 2892 (2001).
[9] Claude Ederer and Nicola A. Spaldin, Curr. Opin. Solid State Mater. Sci. **9**, 128 (2006).
[10] Spaldin's picture is that the transition metal is ionized into a formally d^0 state which obviously cannot be magnetic and then the O $2p$ electrons form covalent bonds with the empty d states. Formal valencies are extremely predictive, yet are often unrelated to the actual charge distribution in a crystal. We therefore prefer our picture which is that the TM d and O $2p$ states are

nearly degenerate (so no ionization) and a large Hamiltonian matrix element splits them into bonding and antibonding states. The reason they are not magnetic is essentially the same as the reason that the molecular bonds in H_2 are not. A similar point of view is expressed by R. E. Cohen, Nature (London) **358**, 136 (1992). Several polarization mechanisms are discussed by D. I. Khomskii, J. Magn. Magn. Mater. **306**, 1 (2006).

[11] F. Sugawara, S. Iida, Y. Syono, and S. Akimoto, J. Phys. Soc. Jpn. **25**, 1553 (1968).

[12] B. B. van Aken, T. T. M. Palstra, A. Filippetti, and N. A. Spaldin, Nat. Mater. **3**, 164 (2004).

[13] T. Shishidou, N. Mikamo, Y. Uratani, F. Ishii, and T. Oguchi, J. Phys.: Condens. Matter **16**, S5677 (2004).

[14] Craig J. Fennie and Karin M. Rabe, Phys. Rev. B **72**, 100103(R) (2005).

[15] A. A. Belik, S. Iikubo, T. Yokosawa, K. Kodama, N. Igawa, S. Shamoto, M. Azuma, M. Takano, K. Kimoto, Y. Matsui, and E. Takayama-Muromachi, J. Am. Chem. Soc. **129**, 971 (2007). See this paper for references to earlier results.

[16] E. Montanari, G. Calestani, L. Righi, E. Gilioli, F. Bolzoni, K. S. Knight, and P. G. Radaelli, arXiv:cond-mat/07043548.

[17] A. M. dos Santos, S. Parashar, A. R. Raju, Y. S. Zhao, A. K. Cheetham, and C. N. R. Rao, Solid State Commun. **122**, 49 (2002).

[18] R. D. King-Smith and David Vanderbilt, Phys. Rev. B **47**, 1651 (1993).

[19] J. Wang, J. B. Neaton, H. Zheng, V. Nagarajan, S. B. Ogale, B. Liu, D. Viehland, V. Vaithyanathan, D. G. Scholm, U. V. Waghmare, N. A. Spaldin, K. M. Rabe, M. Wuttig, and R. Ramesh, Science **229**, 1719 (2003).

[20] K. Y. Yun, D. Ricinschsi, T. Kanashima, M. Noda, and M. Okuyama, J. Korean Phys. Soc. **46**, 281 (2005).

[21] J. B. Neaton, C. Ederer, U. V. Waghmare, N. A. Spaldin, and K. M. Rabe, Phys. Rev. B **71**, 014113 (2005).

[22] M. Azuma, K. Takata, T. Saito, S. Ishiwata, Y. Shimakawa, and M. Takano, J. Am. Chem. Soc. **127**, 8889 (2005).

[23] M. Sakai, A. Masuno, D. Kan, M. Hashisaka, K. Takata, M. Azuma, M. Takano, and Y. Shimakawa, Appl. Phys. Lett. **90**, 072903 (2007).

[24] Y. Uratani, T. Shishidou, F. Ishii, and T. Oguchi, Physica B **383**, 9 (2006).

[25] P. E. Blöchl, Phys. Rev. B **50**, 17953 (1994).

[26] G. Kresse and J. Furthmuller, Phys. Rev. B **54**, 11169 (1996).

[27] J. P. Perdew, K. Burke, and M. Ernzerhof, Phys. Rev. Lett. **77**, 3865 (1996).

[28] Priya Mahadevan, Alex Zunger, and D. D. Sarma, Phys. Rev. Lett. **93**, 177201 (2004).

[29] O. Bengone, M. Alouani, P. Blochl, and J. Hugel, Phys. Rev. B **62**, 16392 (2000).

[30] This assumption is not really valid because U is a screened Coulomb integral and the screening depends on the environment.

[31] The radii of the projection spheres around each kind of atom are 1.635 Å for Bi, 1.323 Å for Mn, 1.085 Å for Ni, and 0.900 Å for O.

[32] Charles Kittel, *Introduction to Solid State Physics*, 7th ed. (Wiley, New York, 1996), Table 3.9.